XL CILAMCE
IBERO-LATIN AMERICAN CONGRESS ON COMPUTATIONAL METHODS IN ENGINEERING
NOVEMBER 11-14, 2019
Praiamar Natal Hotel & Convention
Natal, RN-BRAZIL

MODAL PARAMETER IDENTIFICATION OF A RECTANGULAR BEAM USING EXPERIMENTAL AND OUTPUT-ONLY MODAL ANALYSES

Luíza da C. Albuquerque
Ulisses A. Monteiro
Ricardo H. Gutiérrez
Jairo A. Huamani
Luiz A. Vaz
luiza.albuquerque@poli.ufrj.br
ulisses@oceanica.ufrj.br
rhramirez@oceanica.ufrj.br
alvarocotaquispe@gmail.com
vaz@oceanica.ufrj.br
Laboratory of Dynamic Tests and Vibration Analysis (LEDAV), Ocean Engineering Program (PENO), Federal University of Rio de Janeiro (UFRJ),
Av. Athos da Silveira Ramos - 149, 21941-909, Rio de Janeiro/RJ, Brasil

Abstract. In order to obtain the modal parameters of a structure, different approaches can be used: (i) Experimental Modal Analysis (EMA), which uses excitation (input) and response (output) data; (ii) Output-Only Modal Analysis (O-OMA), which uses only the output. Both techniques are widely used and their advantages and disadvantages are known. The EMA allows performing a full numerical validation, because the estimated modal matrix is already mass normalized. In the O-OMA case, since the excitation force is unmeasured, the estimated modal matrix can only be normalized to unity. This paper aims to identify the modal parameters of a rectangular beam, simulating "free-free" boundary condition in the excitation's direction. The beam was instrumented with 9 accelerometers equidistantly arranged along the length and the excitation was through a multiple reference impact testing. The modal parameters were identified using the Polyreference Least Square Complex Frequency Domain method, considering two approaches: (i) EMA and (ii) O-OMA methods. Results from the EMA and O-OMA showed that the discrepancies between the natural frequencies were at most 0.5%, and all the vibration modes presented MAC values higher than 0.9. Experimental results were also compared with those obtained through a finite element model of the rectangular beam, showing small differences both in the natural frequencies and vibration modes. It is therefore concluded that the two approaches lead to good estimates of natural frequencies. As for the vibration modes, the modal matrices obtained by the two methods present a small difference, since the mass of the beam is small.

Keywords: Output-Only Modal Analysis (O-OMA), Multiple Reference Impact Testing (MRIT); Polyreference Least Square Complex Frequency Domain (p-LSCF).

1 Introduction

In engineering, the study of vibrations is extremely important, after all, any kind of structure is subject excitations by external forces. The vibrations can be caused, for example, by motors, fluids, winds, and waves, especially in the cases of ships and platforms. In some cases, the source of excitation, the input, is known, but in many cases, it is not possible to measure its value. Therefore, Experimental Modal Analysis (EMA) and Output-Only Modal Analysis (O-OMA) which aims at estimating the modal parameters (vibration modes, damping ratios and natural frequency), are vital to subsequent studies to prevent and prolong the life of any type of structure, minimizing the effects of fatigue and avoiding resonance (Zhi-Fang and Fu [1].

It is possible to estimate the modal parameters with EMA or O-OMA methodologies, regardless of the fact that the input excitation is not known for O-OMA. Examples of these estimates can be found in Orlowitz and Brandt [2]. Eventually, an analysis that uses excitation and output (vibration) measurements may be seem more reliable, since if the excitations are known, it is possible to do a full numerical validation. However, an analysis performed only with output measurements becomes more versatile, after all, it can be performed during a normal operation routine of a structure/equipment where, in many cases, the excitation forces are not known in advance.

Theoretically, the modal parameters estimated by EMA and O-OMA techniques should be similar, unless the normalization of the modal matrices. In this work, to evaluate the results of using these two methodologies, an impact test was performed in an aluminum rectangular beam. During this experiment, care was taken to avoid influences from the external environment.

The vibration time series obtained in the experiment were processed using the Polyreference Least Square Complex Frequency Domain (p-LSCF) method for EMA and O-OMA cases, thus obtaining natural frequencies, damping ratios and mode shapes estimates. Mode shapes were compared using MAC criterion. A finite element model (FEM) of the rectangular beam was developed and used for comparison purpose, at this research stage. In the future it will be used for performing model calibration.

2 Polyreference Least Square Complex Frequency Domain (p-LSCF)

The Least-Squares Complex Frequency-domain (LSCF) estimator can be viewed as a frequency-domain implementation of the well-known Least-Squares Complex Exponential (LSCE) estimator. In this paper, the LSCF estimator used is a "poly-reference" estimator (p-LSCF), which means that a so-called Right Matrix-Fraction Description (RMFD) was used to estimate the modal participation factor and the poles directly, as described in Peeters *et al.* [3].

2.1 Poles and Modal Participation Factors Estimation

According to Peeters *et al.* [3], the relationship between output "*o*" ($o = 1,\ldots,N_o$) and input "*i*" ($i = 1,..,N_i$) can be modeled in the frequency domain by means of right matrix-fraction description (RMFD) as Peeters et al. [3]:

$$\mathbf{H}_{\boldsymbol{o}}(\omega) = \mathbf{N}_o(\omega)\mathbf{D}^{\mathbf{-1}}(\omega) \tag{1}$$

With the numerator row-vector polynomial of output "*o*":

$$\mathbf{N}_o(\omega) = \sum_{j=0}^{n} \boldsymbol{\Omega}_j(\omega)\mathbf{B}_{oj} \tag{2}$$

And the denominator matrix polynomial:

$$\mathbf{D}(\omega) = \sum_{j=0}^{n} \boldsymbol{\Omega}_j(\omega)\mathbf{A}_j \tag{3}$$

Several choices are possible for the polynomial basis $\mathbf{\Omega}_j(\omega)$. For a discrete-time domain model, functions $\mathbf{\Omega}_j(\omega)$ are usually given by:

$$\mathbf{\Omega}_j(\omega) = e^{-i\omega T_s \cdot j} \tag{4}$$

Where T_s is the sampling period. The matrix coefficients $\mathbf{A}_j$ and $\mathbf{B}_{oj}$ are the parameters to be estimated. All these coefficients are grouped together in one matrix $\boldsymbol{\theta} = \left[\boldsymbol{\beta}_1^{\mathrm{T}}, \ldots, \boldsymbol{\beta}_{\mathrm{N}_0}^{\mathrm{T}}, \boldsymbol{\alpha}^{\mathrm{T}}\right]^{\mathrm{T}}$ with:

$$\mathbf{B}_{oj} = \begin{Bmatrix} \mathbf{B}_{o0} \\ \mathbf{B}_{o1} \\ \cdot \\ \cdot \\ \cdot \\ \mathbf{B}_{on} \end{Bmatrix}, \quad \boldsymbol{\alpha} = \begin{Bmatrix} \mathbf{A}_0 \\ \mathbf{A}_1 \\ \cdot \\ \cdot \\ \cdot \\ \mathbf{A}_n \end{Bmatrix} \tag{5}$$

Estimates of the transfer-function matrix coefficients can be obtained by minimizing the weighted nonlinear least-squares (NLS) cost function with respect to the parameter matrix $\boldsymbol{\theta}$. However, this WNLS problem can be approximated by a (sub-optimal) weighted linear least-squares (WLS) one, which is found by minimizing the cost function (Peeters *et al.* [3]):

$$\mathrm{C}_{LS}(\boldsymbol{\theta}) = \sum_{o=1}^{\mathrm{N}_0} \mathrm{tr}\left(\left(\boldsymbol{\varepsilon}_0^{LS}(\boldsymbol{\theta})\right)^H \cdot \boldsymbol{\varepsilon}_0^{LS}(\boldsymbol{\theta})\right) \tag{6}$$

With tr(·) the trace operator and where the (weighted) LS equation error, $\boldsymbol{\varepsilon}_0^{LS}(\boldsymbol{\theta})$, which is linear in the parameters, is a row-vector defined as:

$$\boldsymbol{\varepsilon}_0^{LS}(\omega_f, \boldsymbol{\theta}) \stackrel{\mathrm{def}}{=} \boldsymbol{\varepsilon}_0^{LS}(\boldsymbol{\theta}) = W_o(\omega_f) \sum_{j=0}^{n} \left(\mathbf{\Omega}_j(\omega_f)\mathbf{B}_{oj} - \mathbf{\Omega}_j(\omega_f)\mathbf{H}_{\boldsymbol{o}}(\omega_f)\mathbf{A}_j\right) \tag{7}$$

With $W_o(\omega_f)$ an arbitrary weighting function and $\mathbf{H}_{\boldsymbol{o}}(\omega_f)$ the o-th row of the FRF matrix. Eq. (7) can be reformulated in matrix notation as:

$$\boldsymbol{\varepsilon}_0^{LS}(\boldsymbol{\theta}) = \begin{Bmatrix} \boldsymbol{\varepsilon}_0^{LS}(\omega_1, \boldsymbol{\theta}) \\ \vdots \\ \boldsymbol{\varepsilon}_0^{LS}(\omega_{N_f}, \boldsymbol{\theta}) \end{Bmatrix} = [\mathbf{X}_o \quad \mathbf{Y}_o] \cdot \begin{Bmatrix} \boldsymbol{\beta}_{\boldsymbol{o}} \\ \boldsymbol{\alpha} \end{Bmatrix} \tag{8}$$

With:

$$\mathbf{X}_o = \begin{bmatrix} (W_o(\omega_1)[\mathbf{\Omega}_0(\omega_1) \cdots \mathbf{\Omega}_n(\omega_1)]) \otimes \mathbf{I}_{N_i} \\ \vdots \\ \left(W_o(\omega_{N_f})\left[\mathbf{\Omega}_0(\omega_{N_f}) \cdots \mathbf{\Omega}_n(\omega_{N_f})\right]\right) \otimes \mathbf{I}_{N_i} \end{bmatrix} \tag{9}$$

$$\mathbf{Y}_o = \begin{bmatrix} -(W_o(\omega_1)[\mathbf{\Omega}_0(\omega_1) \cdots \mathbf{\Omega}_n(\omega_1)]) \otimes \mathbf{H}_{\boldsymbol{o}}(\omega_1) \\ \vdots \\ -\left(W_o(\omega_{N_f})\left[\mathbf{\Omega}_0(\omega_{N_f}) \cdots \mathbf{\Omega}_n(\omega_{N_f})\right]\right) \otimes \mathbf{H}_{\boldsymbol{o}}(\omega_{N_f}) \end{bmatrix} \tag{10}$$

Therefore, Eq. (6) can be rewritten as:

$$\mathrm{C}_{LS}(\boldsymbol{\theta}) = \sum_{o=1}^{\mathrm{N}_0} \mathrm{tr}\left([\boldsymbol{\beta}_o^T \quad \boldsymbol{\alpha}^T] \cdot \begin{bmatrix} \mathbf{R}_{\boldsymbol{o}} & \mathbf{S}_{\boldsymbol{o}} \\ \boldsymbol{S}_{\boldsymbol{o}}^T & \mathbf{T}_{\boldsymbol{o}} \end{bmatrix} \cdot \begin{Bmatrix} \boldsymbol{\beta}_{\boldsymbol{o}} \\ \boldsymbol{\alpha} \end{Bmatrix}\right) \tag{11}$$

With $\mathbf{R}_{\boldsymbol{o}} = Re(\mathbf{X}_o^T \mathbf{X}_o)$, $\mathbf{S}_{\boldsymbol{o}} = Re(\mathbf{X}_o^T \mathbf{Y}_o)$ and $\mathbf{T}_{\boldsymbol{o}} = Re(\mathbf{Y}_o^H \mathbf{Y}_o)$.

When the cost function (Eq. (11)) is minimum, the derivatives of with respect to the unknown matrix coefficients $\boldsymbol{\beta}_{\boldsymbol{o}}$ and $\boldsymbol{\alpha}$ will be zero, which leads to:

$$\mathbf{M} \cdot \boldsymbol{\alpha} = \mathbf{0} \tag{12}$$

With:

$$\mathbf{M} = \left[2 \sum_{o=1}^{N_0} \left(\mathbf{T}_o - \boldsymbol{S}_o^T \boldsymbol{R}_o^{-1} \mathbf{S}_o \right) \right] \tag{13}$$

To remove the parameter redundancy of the RMFD transfer function model, Eq. (1), a constraint has to be imposed on the matrix coefficients. For instance, by imposing that the last matrix coefficient of $\boldsymbol{\alpha}$ is constrained to the identity matrix.

Once $\widehat{\boldsymbol{\alpha}}_{LS}$, the least-squares estimate of $\boldsymbol{\alpha}$, is known, $\widehat{\boldsymbol{\beta}}_o = -\boldsymbol{R}_o^{-1}\mathbf{S}_o \cdot \widehat{\boldsymbol{\alpha}}_{LS}$, can be used to derive all $\widehat{\boldsymbol{\beta}}_{LS,o}$ matrix coefficients. From the knowledge of the denominator matrix coefficients it is now possible to compute the poles and corresponding modal participation factors by computing the eigenvalue decomposition of the so-called companion matrix (Peeters *et al.* [3]).

2.2 Mode Shape Estimation

Once the poles (λ_m) together with the modal participation factors ($\mathbf{L}_m$) have been determined by means of a stabilization diagram, the well-known Least-Squares Frequency-Domain (LSFD) estimator can be used to directly estimate the mode shapes, $\boldsymbol{\Psi}_m$, (Peeters *et al.* [3]) occurring in:

$$\mathbf{H}(s) = \sum_{m=1}^{N_m} \left(\frac{\boldsymbol{\Psi}_m \cdot \mathbf{L}_m^T}{s - \lambda_m} + \frac{\boldsymbol{\Psi}_m^* \cdot \mathbf{L}_m^H}{s - \lambda_m^*} \right) + \frac{\mathbf{LR}}{s^2} + \mathbf{UR} \tag{14}$$

Where **LR** is the lower residue, **UR** is the upper residue, N_m is the number of modes; λ_m is the mth pole, and are related to the damping factor (σ_m), damped modal frequency (ω_{dm}) and modal damping ratio (ζ_m) as given in Eq. (15):

$$\lambda_m = -\sigma_m + i\omega_{dm}\,;\ \omega_m = \sqrt{\sigma_m^2 + \omega_{dm}^2};\ \zeta_m = \frac{\sigma_m}{\sqrt{\sigma_m^2 + \omega_{dm}^2}} \tag{15}$$

3 Experimental Procedure

The objective of the experiment described in this article was to measure the inputs (excitation forces) and outputs (vibration responses) due to the impacts in a rectangular test beam. For this, the following equipment was used:

- 01 B&K Model 8200 Impact Hammer (10.2 mV / N)
- 09 Uniaxial Accelerometers (6 Kistlers, 2 Kjaer and 1 PCB)
- A National Instruments Model NI 92334 Data Acquisition Card

Table 1 presents the dimensional data of the rectangular aluminum beam.

Table 1. Aluminum beam dimensions

Dimensions	Data
Thickness	6.17 mm
Width	25.42 mm
Length	2145 mm

The nine accelerometers were equally distributed and attached to the test beam used, with a distance of 268 mm between them. This arrangement is shown in Fig. 1. The test was performed using an impact hammer with a steel tip, which is best suited for the frequency range. The analysis was limited to the range between 0 to 200 Hz, where 7 vibration modes were identified. The impacts were directed at the accelerometers position arranged on the test beam, defining the 09 degrees of freedom.

During the experiment, care was taken to prevent beam movements and from being restricted in the direction of impact, as the purpose was to represent the beam boundary condition as free-free.

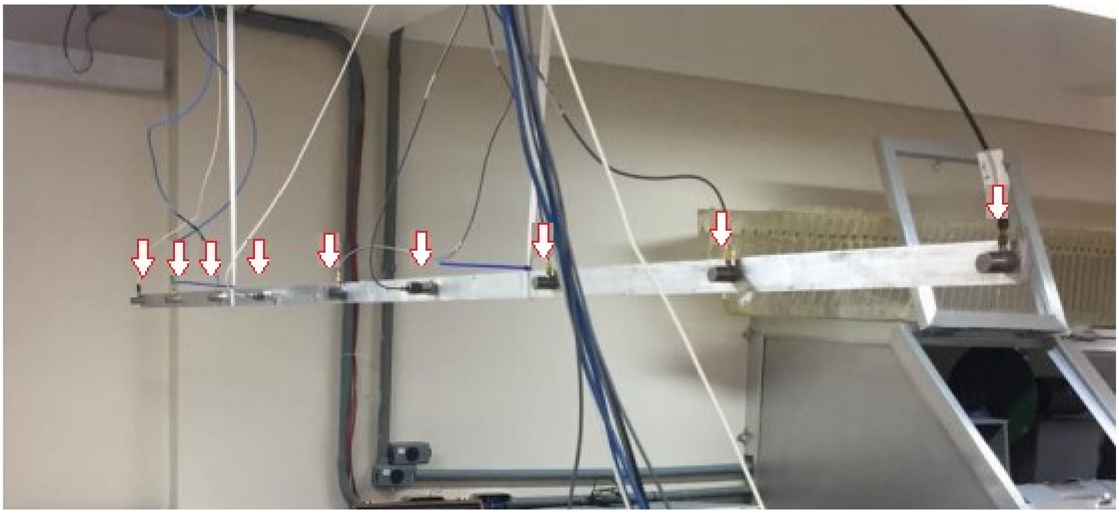

Figure 1. Rectangular aluminum beam used instrumented with 9 uniaxial accelerometers

4 Result Analysis and Discussion

The vibration time series obtained were processed using the LSCF method described in section 2. Natural frequency, damping ratios and mode shapes were estimate. In Table 2, results obtained for natural frequency and damping ratios are presented, for EMA and O-OMA, in the range between 0 and 200 Hz. Table 1 also provides a comparison between the estimation obtained by O-OMA and EMA analyses.

Table 2. Comparison between modal parameters obtained using the LSCF method for O-OMA and EMA analyses

	O-OMA		**EMA**		**Difference (%)**	
Vibration Modes	f_n **[Hz]**	ζ_n **[%]**	f_η **[Hz]**	ζ_n **[%]**	f_n	ζ_n
1	6.324	1.84	6.326	1.82	0.03%	1.09%
2	17.592	1.39	17.592	1.28	0.00%	7.91%
3	34.035	0.44	34.205	0.57	0.49%	22,8%
4	56.623	0.75	56.846	0.67	0.39%	10.67%
5	84.608	0.61	84.811	0.69	0.24%	13.12%
6	119.381	0.38	119.407	0.35	0.02%	7.90%
7	153.972	0.26	153.986	0.31	0.01%	19.23%

In relation to the natural frequencies, it can be seen that the differences between results found using EMA and O-OMA are not larger than 1%, as shown in table 1.

Regarding the experimentally obtained damping ratios, it can be seen that the differences is considerably larger than those of natural frequencies. It is known that damping ratios estimation are much more susceptible to noise than the natural frequencies.

Another comparison was made using a FEM of the rectangular beam. Table 3 shows the natural frequencies calculated for a simple beam in free-free boundary condition. It also shows the difference between FEM and O-OMA results.

Table 3. Comparison between natural frequencies obtained using O-OMA and FEM analyses

	FEM	**O-OMA**	**Difference (%)**
Vibration Modes	f_n **[Hz]**	f_n **[Hz]**	f_n **[Hz]**
1	6.26	6.324	1.02%
2	17.528	17.592	0.37%
3	34.43	34.035	1.15%
4	56.966	56.623	0.60%
5	85.136	84.608	0.62%
6	118.94	119.381	0.37%
7	153.996	153.972	0.02%

Table 4 shows the natural frequencies calculated for a simple beam in free-free boundary condition. It also shows the difference between FEM and EMA results.

It can be noted that all natural frequencies in the frequency range of 0 to 200 Hz were experimentally identified, mainly because the hammer tip material used was suitable for the desired frequency range.

Table 4. Comparison between natural frequencies obtained using EMA and FEM analyses

	FEM	**EMA**	**Difference (%)**
Vibration Modes	f_n **[Hz]**	f_n **[Hz]**	f_n **[Hz]**
1	6.26	6.326	1.05%
2	17.528	17.592	0.37%
3	34.43	34.205	0.65%
4	56.966	56.846	0.21%
5	85.136	84.811	0.38%
6	118.94	119.407	0.39%
7	153.996	153.986	0.01%

It can also be observed that the largest difference between the natural frequencies obtained by experimental and FEM analyses is 1.15%, as shown in Tables 3 and 4. This difference can be attributed to modeling issues and can be corrected by numerical model calibration.

The mode shapes obtained using O-OMA, EMA, FEM and analytical analyses are presented in Fig. (2). It is possible to visually compare the results and see that experimental mode shapes are well correlated to the numerical and analytical ones.

A small difference in mode shapes amplitudes can be seen in Fig. (2) between EMA (in blue) and O-OMA (in red) results. This is because the modal matrix from EMA analysis is already mass-normalized, while the modal matrix from O-OMA analysis is normalized to unity. For this reason, mode shapes from O-OMA analysis cannot be used for load estimation, for instance, unless mass-normalization are done.

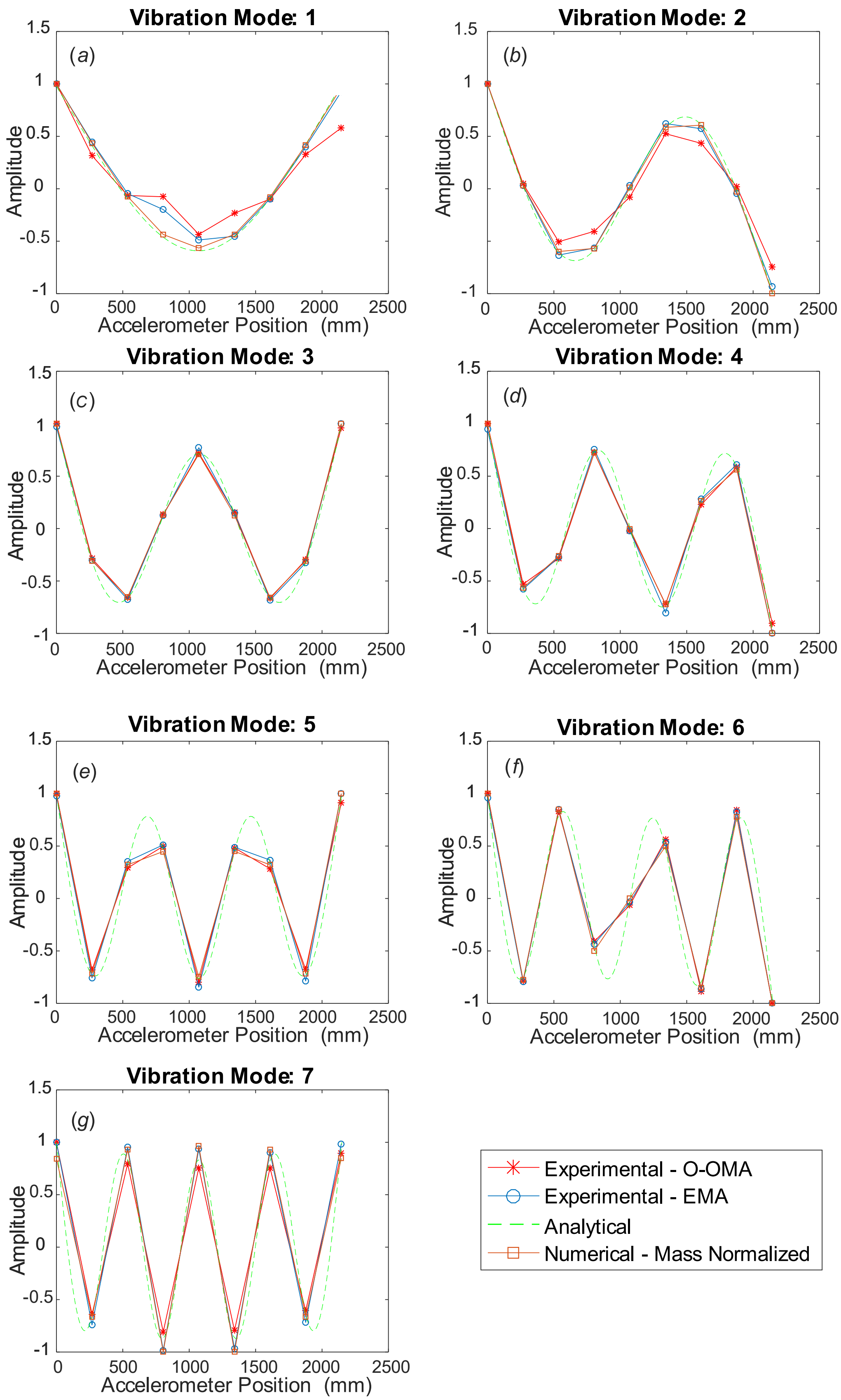

Figure 2. Mode shapes obtained using O-OMA, EMA, FEM and analytical analyses

By analyzing the vibration modes found experimentally (with EMA and O-OMA) and those obtained from the numerical model, it is noted that all seven mode shapes are well correlated. This statement can also be verified by noting high MAC values in the main diagonal of Fig. (3a,b,c), normally greater than 0.9 and lower values in the off-diagonal elements, typically below 0.1.

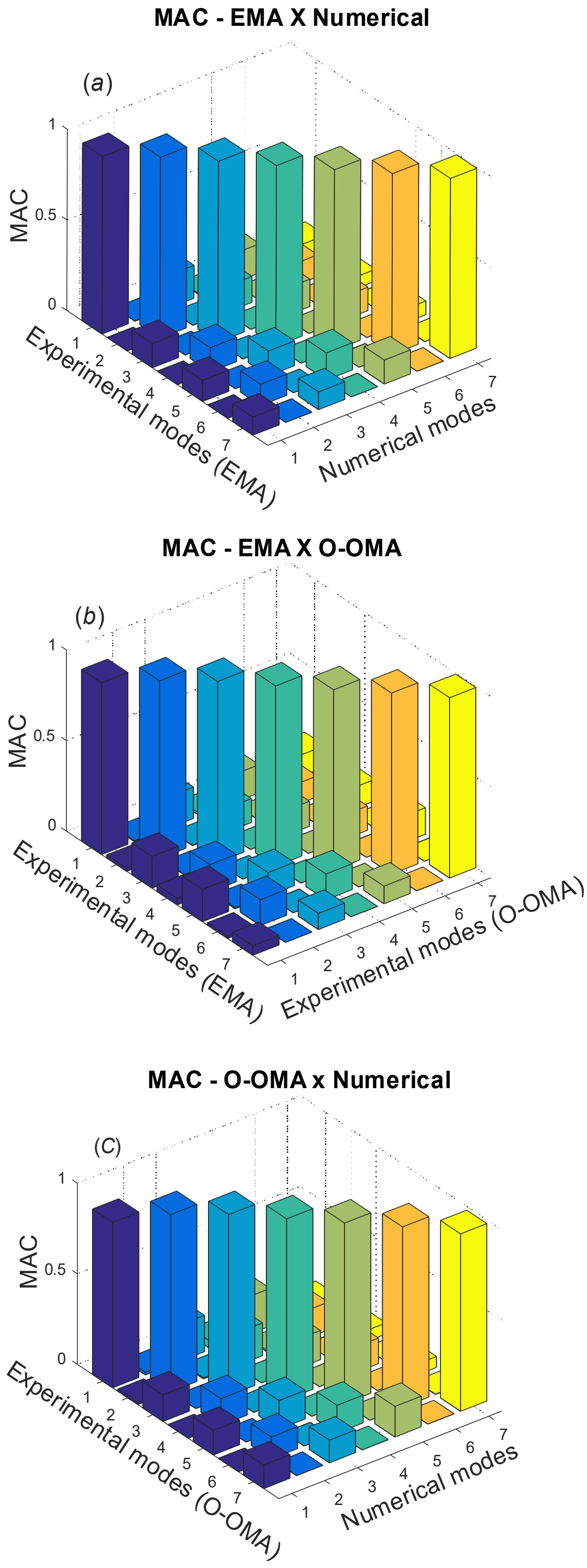

Figure 3. MAC Chart for mode shapes comparison

5 Conclusion

After performing impact test experiment using a rectangular beam, two types of modal analysis methodologies were used in order to estimate the modal parameters: one using only the output vibration measurement, and another using the input (force excitation) and output (vibration) measurement. After, a comparison was made between their results. In this comparison, it is noted that the difference between the natural frequency estimations of both analyses does not exceed 1%. So, it can be concluded that both methodologies, EMA and O-OMA, have the same level of precision in calculating natural frequencies.

Regarding the damping ratios, it can be seen that the differences are bigger between the two methodologies. It is known that damping is more susceptible to measurement noises and still the object of many researches.

In addition, a numerical model was also used in order to obtain another comparison criterion. It is observed that the largest difference (for natural frequency) between experimental analysis and numerical model is 1.15%. As this value can be considered negligible, it was concluded that the numerical model results were compatible with the experimental estimations, thus considering that model valid.

Regarding the vibration modes, when making a comparison using MAC as a criterion, we see that the mode shapes from experimental analyses and those from the numerical model are all well correlated with each other, since all have MAC values greater than 0.9. Vibration modes from the EMA and O-OMA analyses show a small difference in their amplitude, and this can be explained as modal matrix from EMA are already mass-normalized, whereas the modal matrix from O-OMA is normalized to unity.

Finally, it can be concluded that EMA and O-OMA analyses have the same precision in calculating natural frequencies, but caution must be used when using results from damping ratios (for both methods) and the modal matrix from O-OMA tests.

Acknowledgements

This study was possible due to sponsorship of Petrobras through its Research and Development Center (CENPES), under Grant 5850.0106375.17.9.

The experimental apparatus was assembled by Mr. Hualber Berbet and the data acquisition software was developed by Mr. Frederico Novaes (M.Sc), both from the dynamic testing and vibration analysis laboratory (LEDAV/COPPE/UFRJ).

References

[1] Zhi-Fang Fu JH. Modal Analysis. 2001.

[2] Orlowitz E, Brandt A. Comparison of experimental and operational modal analysis on a laboratory test plate. Meas J Int Meas Confed 2017;102:121–30. doi:10.1016/j.measurement.2017.02.001.

[3] Peeters B, Van der Auweraer H, Guillaume P, Leuridan J. The PolyMAX Frequency-Domain Method: A New Standard for Modal Parameter Estimation? Shock Vib 2004;11:395–409. doi:10.1155/2004/523692.